The EMBO Journal (2011) 30, 2294–2305 | © 2011 European Molecular Biology Organization | All Rights Reserved 0261-4189/11
www.embojournal.org

THE EMBO JOURNAL

Galactose-modified iNKT cell agonists stabilized by an induced fit of CD1d prevent tumour metastasis

Sandrine Aspeslagh[1,6], Yali Li[2,6], Esther Dawen Yu[2], Nora Pauwels[3], Matthias Trappeniers[3], Enrico Girardi[2], Tine Decruy[1], Katrien Van Beneden[1], Koen Venken[1], Michael Drennan[1], Luc Leybaert[4], Jing Wang[2], Richard W Franck[5], Serge Van Calenbergh[3], Dirk M Zajonc[2,*] and Dirk Elewaut[1,*]

[1]Department of Rheumatology, Faculty of Medicine and Health Sciences, Laboratory for Molecular Immunology and Inflammation, Ghent University, Ghent, Belgium, [2]Division of Cell Biology, La Jolla Institute for Allergy and Immunology, La Jolla, CA, USA, [3]Faculty of Pharmaceutical Sciences, Laboratory for Medicinal Chemistry, Ghent University, Ghent, Belgium, [4]Department of Basic Medical Sciences-Physiology Group, Faculty of Medicine and Health Sciences, Ghent University, Ghent, Belgium and [5]Department of Chemistry, Hunter College of CUNY, New York City, NY, USA

Invariant natural killer T (iNKT) cells are known to have marked immunomodulatory capacity due to their ability to produce copious amounts of effector cytokines. Here, we report the structure and function of a novel class of aromatic α-galactosylceramide structurally related glycolipids with marked Th1 bias in both mice and men, leading to superior tumour protection *in vivo*. The strength of the Th1 response correlates well with enhanced lipid binding to CD1d as a result of an induced fit mechanism that binds the aromatic substitution as a third anchor, in addition to the two lipid chains. This induced fit is in contrast to another Th1-biasing glycolipid, α-C-GalCer, whose CD1d binding follows a conventional key-lock principle. These findings highlight the previously unexploited flexibility of CD1d in accommodating galactose-modified glycolipids and broaden the range of glycolipids that can stimulate iNKT cells. We speculate that glycolipids can be designed that induce a similar fit, thereby leading to superior and more sustained iNKT cell responses *in vivo*.

The EMBO Journal (2011) **30,** 2294–2305. doi:10.1038/emboj.2011.145; Published online 6 May 2011
Subject Categories: immunology; structural biology
Keywords: CD1d; glycolipids; iNKT cells

*Corresponding authors. DM Zajonc, Division of Cell Biology, La Jolla Institute for Allergy and Immunology, 9420 Athena Circle, La Jolla, CA 92037, USA. Tel.: +1 858752 6605; Fax: +1 858752 6985; E-mail: dzajonc@liai.org or D Elewaut, Department of Rheumatology, Laboratory for Molecular Immunology and Inflammation, Ghent University, De Pintelaan 185, 9000 Ghent, Belgium. Tel.: +32 (9)3322240; Fax: +32 (9)3323803; E-mail: Dirk.Elewaut@ugent.be
[6]These authors contributed equally to this work

Received: 30 January 2011; accepted: 14 April 2011; published online: 6 May 2011

Introduction

Invariant natural killer T (iNKT) cells form a subset of regulatory T cells with features of both innate and adaptive immunity. In contrast to conventional T cells that are activated by a peptide presented by an MHC class I or II molecule, iNKT cells recognize lipid derivatives present in the context of CD1d, a non-classical MHC I molecule expressed on antigen presenting cells (APCs) (Godfrey *et al*, 2004).

The list of CD1d binding glycolipids that can activate iNKT cells is consistently growing and contains different endogenous and exogenous glycolipids. The latter includes very diverse microbial glycolipids and synthetically derived compounds, of which α-galactosylceramide (α-GalCer) is a prototypical glycolipid antigen. α-GalCer consists of a galactose head group that is α-anomerically linked to a phytoceramide, which is composed of a phytosphingosine chain coupled to an acyl chain. The crystal structures of both mouse and human CD1d bound to α-GalCer show that both alkyl chains fit into two pockets of CD1d, the F′ and A′ pocket, while the galactose is exposed at the CD1d surface for interaction with the TCR (Koch *et al*, 2005; Zajonc *et al*, 2005a). The invariant α chain of the TCR recognizes the sugar moiety, whereas the TCR-β chain interacts with CD1d residues. However, in contrast to conventional T cells, the complementarity determining regions of the iNKT TCR do not alter their conformation upon antigen recognition (Borg *et al*, 2007) and appear to be functionally conserved in both mouse and man (Pellicci *et al*, 2009).

In this context, TCR-dependent recognition of α-GalCer results in the robust production of Th1 (e.g., IFN-γ and IL-12), Th2 (e.g., IL-4) and also Th17 cytokines both by iNKT cells itself and by activated bystander cells (Coquet *et al*, 2008). As several pathological processes are characterized by Th1- or Th2-polarized immune responses, much attention has been focused on attempting to skew iNKT cell cytokine responses towards a more Th1- or Th2-biased cytokine profile. Such strategies have been shown to be effective for Th2 analogues such as OCH, which has been shown to improve the outcome of several autoimmune models including experimental autoimmune encephalitis and arthritis (Miyamoto *et al*, 2001; Chiba *et al*, 2004). Conversely, an α-GalCer analogue, in which the oxygen of the glycosidic linkage has been altered to methylene (α-C-GalCer), is known to skew iNKT cell responses towards a Th1 profile and has been applied to the B16 model murine model for melanoma metastasis (Schmieg *et al*, 2003).

Although the underlying mechanisms are currently unclear, several groups have attempted to provide models that explain iNKT cell cytokine polarization. For example, for Th2 analogues such as OCH, the analysis of the crystal structure when bound to CD1d shows the absence of an induced fit above the F′ pocket of CD1d (F′ roof). This has been proposed

to result in a shorter half-life for CD1d–OCH complexes, which may modulate the interaction with the iNKT TCR (Sullivan *et al*, 2010). As a consequence, the ability of iNKT cells to activate accessory cell types such as NK cells is also diminished. For other Th2-polarizing analogues, the ability to directly load CD1d on the surface of cellular membranes was proposed (Bai *et al*, 2009; Im *et al*, 2009). Although α-C-GalCer displayed a reduced TCR avidity similar to OCH *in vitro*, it was shown that the complexes with CD1d were much more stable *in vivo*, which allowed a more sustained activation of iNKT cells (Sullivan *et al*, 2010). This in turn is correlated with its uniquely Th1-biasing properties, such as inducing IL-12 in a CD40L-dependent manner (Fujii *et al*, 2006). Additionally, the role of APCs has been emphasized by the observation that loading of bone marrow dendritic cells (BMDCs) with α-GalCer and α-C-GalCer enhances its Th1-polarizing potencies in contrast to its soluble injection (Fujii *et al*, 2002).

Generally, the currently described Th1- and Th2-biasing α-GalCer analogues, such as α-C-GalCer or OCH, tend to exhibit reduced overall antigenic potencies compared with α-GalCer *in vivo*. Affirmatively, both α-C-GalCer and OCH have been shown to display a relatively weak interaction with CD1d and TCR. Here, we describe that introduction of selected aromatic groups at position 6″ of the galactopyranosyl ring may afford analogues with unique functional features, that is, a strong Th1 polarization and tumour suppression. These interesting properties are believed to result from a reinforced interaction with CD1d, caused by the induction of significant conformational changes in CD1d that allows accommodation of the aromatic ring. These findings highlight an hitherto unknown flexibility of CD1d in accommodating glycolipids by inducing the formation of an additional small pocket on top of the A′ roof, independently of the F′ and A′ pockets, leading to more sustained iNKT cell responses *in vivo* and also broadening the range of glycolipids that can activate iNKT cells.

Results

6″-derivatized α-GalCer analogues induce a marked Th1 polarization

The crystal structure of the hCD1d–α-GalCer–TCR trimolecular complex highlighted the importance of the 2″-OH, 3″-OH and 4″-OH groups of the galactose head group, as all these hydroxyl groups form strong hydrogen bonds with Gly96a, Ser30a and Phe29a located on the human invariant TCR-α chain (Borg *et al*, 2007). The 6″-OH group is the only hydroxyl group not involved in hydrogen bond formation, suggesting the possibility of introducing modifications without the loss of important interactions. Therefore, we generated a series of analogues with aromatic groups connected via different linkages to the C6″ of the galactose group aimed at generating extra hydrophobic interactions. For this study, we selected five novel synthetic glycolipids, structurally related to α-GalCer, comprising the 3-epimer of α-GalCer (xylo-α-GalCer) and four 6″-derivatives (NU-α-GalCer, PhU-α-GalCer, BzNH-α-GalCer and 4ClBzHN-α-GalCer) (Figure 1). Their Th1–Th2 profile was analysed by determining the IFN-γ and IL-4 levels in the serum. NU-α-GalCer, featuring a naphthylurea (NU) substituent, induced serum levels of IFN-γ comparable to α-GalCer combined with markedly reduced IL-4 levels, thereby inducing the most significant Th1 bias from all the studied 6″-derivatives. By contrast, injection with xylo-α-GalCer induces a weak Th2 profile as compared with the conventionally used Th2 polarizer OCH (Miyamoto *et al*, 2001; Chiba *et al*, 2004). Some iNKT cell subsets are known to secrete IL-17 (Coquet *et al*, 2008). However, IL-17 secretion was undetectable in the serum at different time points by any of the studied analogues (data not shown). Furthermore, 6″-derivatives induced also a Th1 cytokine bias in mice of a BALB/c background (data not shown) and this was CD1d dependent (Supplementary Figure S2). Thus, addition of an aromatic moiety at the 6″-position of the galactose moiety leads to a marked functional Th1 polarization *in vivo*.

It has previously been shown that α-GalCer-induced IFN-γ production *in vivo* can be prolonged by loading the glycolipids onto BMDCs (Fujii *et al*, 2002). We therefore investigated whether the Th1 profile induced by NU-α-GalCer could be extended when using NU-α-GalCer-loaded BMDCs. As shown in Figure 1B and Supplementary Figure S1, the IFN-γ response to NU-α-GalCer-pulsed BMDCs is markedly higher compared with α-GalCer, leading to a sustained Th1 bias *in vivo*.

In this context, most iNKT cell-dependent IFN-γ production is derived from NK cell activation in an IL-12-dependent manner (Kitamura *et al*, 1999). In line with this, IL-12 production was found to be markedly elevated for NU-α-GalCer compared with α-GalCer (Figure 1B; Supplementary Figure S2). Furthermore, NU-α-GalCer was also able to induce a Th1-biased cytokine secretion in cultures of human peripheral blood mononuclear cells (PBMCs) (data not shown) and purified human iNKT cells (Figure 1C), highlighting the conserved nature of the Th polarization.

Superior tumour protection of 6′-modified analogues

Encouraged by the fact that IL-12 and IFN-γ are the primary mediators of prevention of lung metastasis in the B16 melanoma model (Kim *et al*, 2000; Kakuta *et al*, 2002; Airoldi *et al*, 2007), we decided to directly test the *in vivo* impact of the Th1 bias elicited by NU-α-GalCer. We therefore evaluated whether the Th1 bias elicited by NU-α-GalCer provided an enhanced protection in the B16 melanoma model when compared with α-GalCer or xylo-α-GalCer, a weak Th2-biasing analogue. In this context, the glycolipids were either directly injected or delivered via BMDCs. When administered directly at high doses, all of the tested glycolipids prevented tumour growth (Figure 2A), whereas at lower doses only NU-α-GalCer, and to a lesser extent α-GalCer, could provide protection (Figure 2A). When glycolipids were loaded onto BMDCs and adoptively transferred, NU-α-GalCer was significantly more potent in preventing tumour growth compared with α-GalCer and xylo-α-GalCer, the latter eliciting very little if any tumour protection under these conditions (Figure 2B and C). When the tumour load was doubled the observed differential effect of NU-α-GalCer versus α-GalCer and xylo-α-GalCer was even more striking (Figure 2D).

Increased calcium flux and IL-2-dependent NKT cell expansion

To further investigate the anti-tumour potency of NU-α-GalCer, we assayed iNKT cell frequency and expansion at

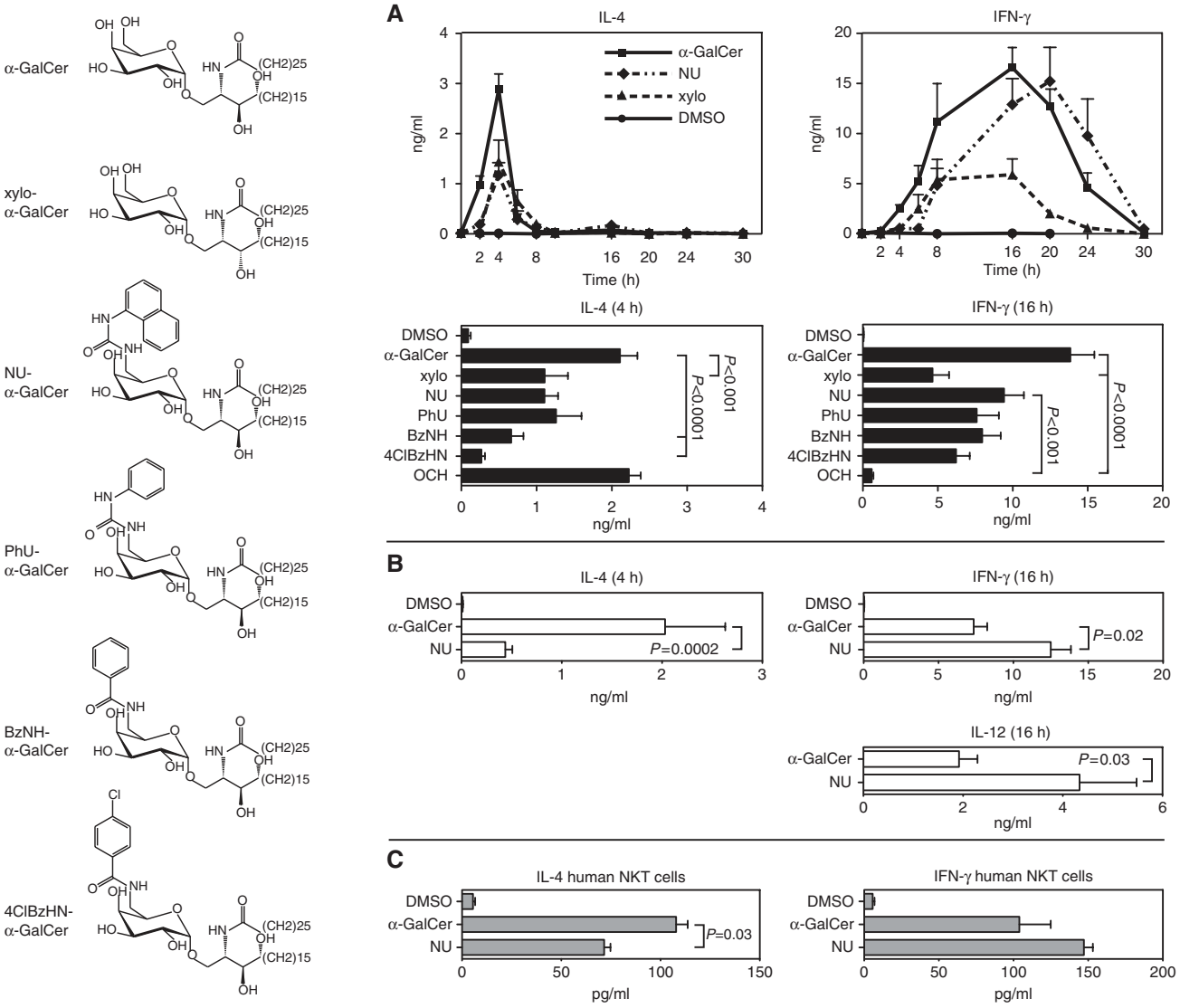

Figure 1 Th1–Th2 profile of novel glycolipids. (**A**) Serum cytokine levels at different time points after injection of 5 μg glycolipid (i.p.). IL-4 levels peak at 4 h whereas IFN-γ levels peak at 16 h after injection (upper panel). Graphs indicate the mean with s.e.m. for at least eight mice. Data are of two independent experiments. Therefore, this analysis was extended to all 6′OH analogues at these time points (lower panel). IFN-γ levels of OCH are significantly lower compared with NU-α-GalCer and α-GalCer (Kruskal–Wallis test, Dunn's multiple comparison post-analysis test). Bars indicate the mean with s.e.m. for 8–16 mice/group. Data are of five independent experiments. (**B**) Serum cytokine levels after injection of glycolipid-pulsed BMDCs. IFN-γ and IL-12 concentration is significantly higher for NU-α-GalCer compared with α-GalCer (two-tailed Mann–Whitney *U*-test). Bars indicate the mean with s.e.m. of 6 mice/group. Data are representative for two independent experiments. (**C**) Cytokine levels in supernatant of co-culture human iNKT cells with glycolipid-loaded irradiated PBMCs. Data represent mean with s.e.m. from four experiments using cells from four different donors (two-tailed Mann–Whitney *U*-test).

several time points after administration of the glycolipid-pulsed BMDCs to mice. Consistent with earlier studies, iNKT expansion could be observed 2 days after transfer of α-GalCer-pulsed BMDCs. Strikingly, NU-α-GalCer induced a more prolonged iNKT cell expansion in both spleen and liver (Figure 3; Supplementary Figure S3). Five days after injection of BMDCs pulsed with NU-α-GalCer, iNKT cell numbers were increased up to 2% of all lymphocytes in spleen and 35% in the liver, representing a nearly six- and two-fold expansion, respectively. To directly evaluate the proliferative capacity of iNKT cells, DNA labelling studies (with BrdU) were performed after adoptive transfer of glycolipid-pulsed BMDCs. Recipients of NU-α-GalCer-pulsed BMDCs had an up to two-fold increase in the BrdU incorporation as opposed to mice injected with α-GalCer-loaded cells, indicating a marked increase in iNKT cell expansion (Figure 3A). We also assessed the impact on human iNKT cell expansion. Here, purified human iNKT cells were labelled with CFSE and co-cultured with PBMCs that had been loaded with NU-α-GalCer or α-GalCer. As was observed in mice *in vivo*, NU-α-GalCer induced an increased CFSE dilution and thus proliferation of human iNKT cells when compared with α-GalCer (Figure 3B) and this NU-α-GalCer-mediated expansion was dependent upon IL-2 (data not shown). Accordingly upon recognition of the NU-α-GalCer–CD1d complex, iNKT cells produce IL-2 in much higher and sustained quantities than the control glycolipids (Figure 4A). Thus, iNKT cell recognition by NU-α-GalCer induces an increased IL-2 secretion as

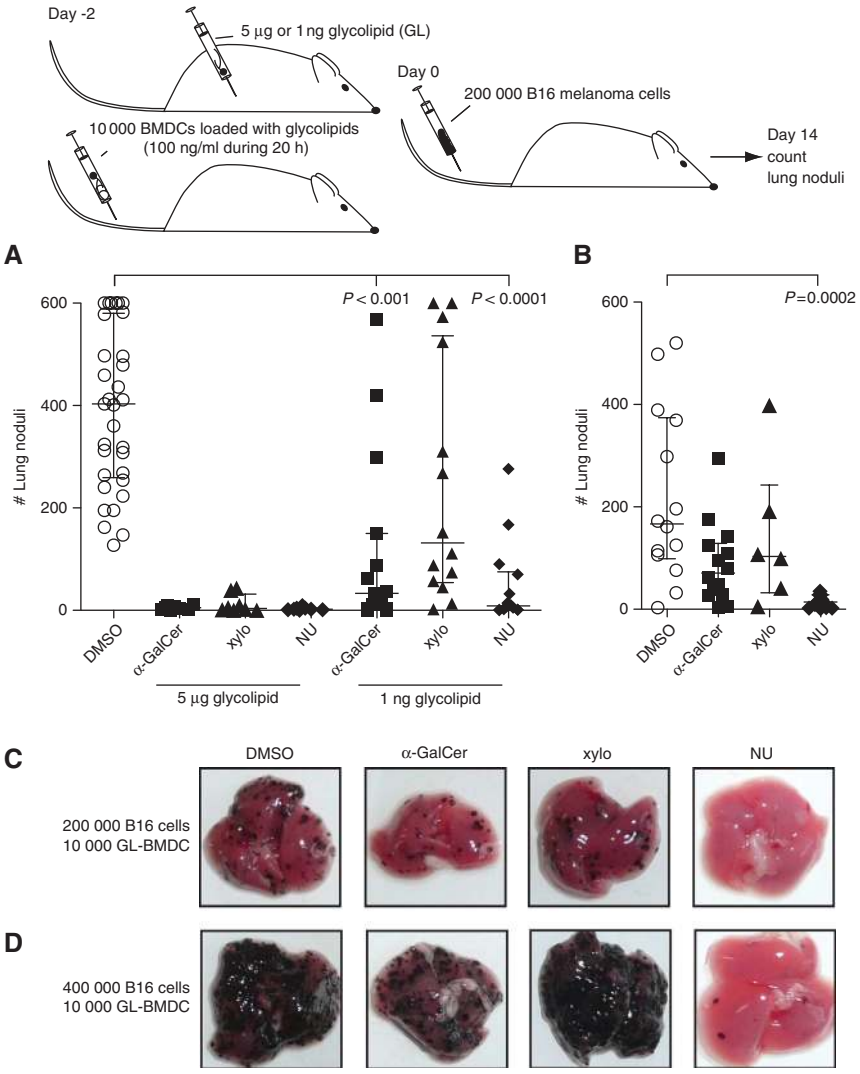

Figure 2 Tumour suppression by iNKT cell stimulation in a B16 melanoma lung metastasis model. (**A**) At 5 μg, there was almost no growth of lung nodules. Both with NU-α-GalCer and α-GalCer, at 1 ng, there is still a significant reduction of the amount of lung nodules. (8 mice/group for 5 μg and 16 mice/group for 1 ng) Data are representative of two independent experiments. (**B**, **C**) When 10 000 BMDCs loaded with glycolipid were injected, NU-α-GalCer was able to reduce the quantity of lung nodules significantly more than α-GalCer. (NU-α-GalCer versus DMSO, $P = 0.0002$). Each dot represents an individual mouse with at least 6 mice/group. Data are representative of two independent experiments. (**D**) The protective effect of BMDCs pulsed with NU-α-GalCer is even more pronounced when the tumour load is increased to 400 000 B16 cells. Error bars express median and interquartile range and a Kruskal–Wallis test (Dunn's multiple comparison post-analysis test) was used for statistical analysis.

compared with α-GalCer and ultimately results in a stronger, iNKT cell proliferation.

Because IL-2 synthesis is triggered by TCR mediated recognition of antigens and subsequent increase of intracellular calcium levels, we focused on calcium flux elicited by iNKT cells after recognition of the glycolipid/CD1d complex. The role of calcium-dependent signals has not been extensively studied in the context of iNKT cells, although it was suggested to be correlated with the formation of a more stable immunological synapse (McCarthy *et al*, 2007) and activation of additional cytokine production (Wang *et al*, 2008). To directly evaluate the impact of the C6′′-modification, we measured intracellular calcium concentration by video microscopy. As indicated in Figure 4, the higher IL-2 production by NU-α-GalCer versus α-GalCer was associated with a marked increase in both the frequency of calcium signalling cells and the calcium signal peak (see also Supplementary videos 1–4).

Differential calcium fluxes elicited by glycolipid ligands may be directly related to a different binding stability of the CD1d–glycolipid–T-cell receptor (McCarthy *et al*, 2007). We therefore focused on the molecular interaction of NU-α-GalCer with mCD1d and the iNKT TCR by surface plasmon resonance (SPR) and crystallography. For comparative purposes, we included the prototypical Th1 analogue α-C-GalCer, as well as the synthetic analogue BnNH-GSL-1′. The latter also possesses an aromatic moiety, which, however, is linked to the sugar via an amide (5′′-CO-NH-) linkage. In that respect it may be considered as an amide derivative of GSL-1′, a galacturonic acid congener of α-GalCer isolated from Sphingomonas species (Kinjo *et al*, 2005). BnNH-GSL-1′ is also a Th1 polarizer, however,

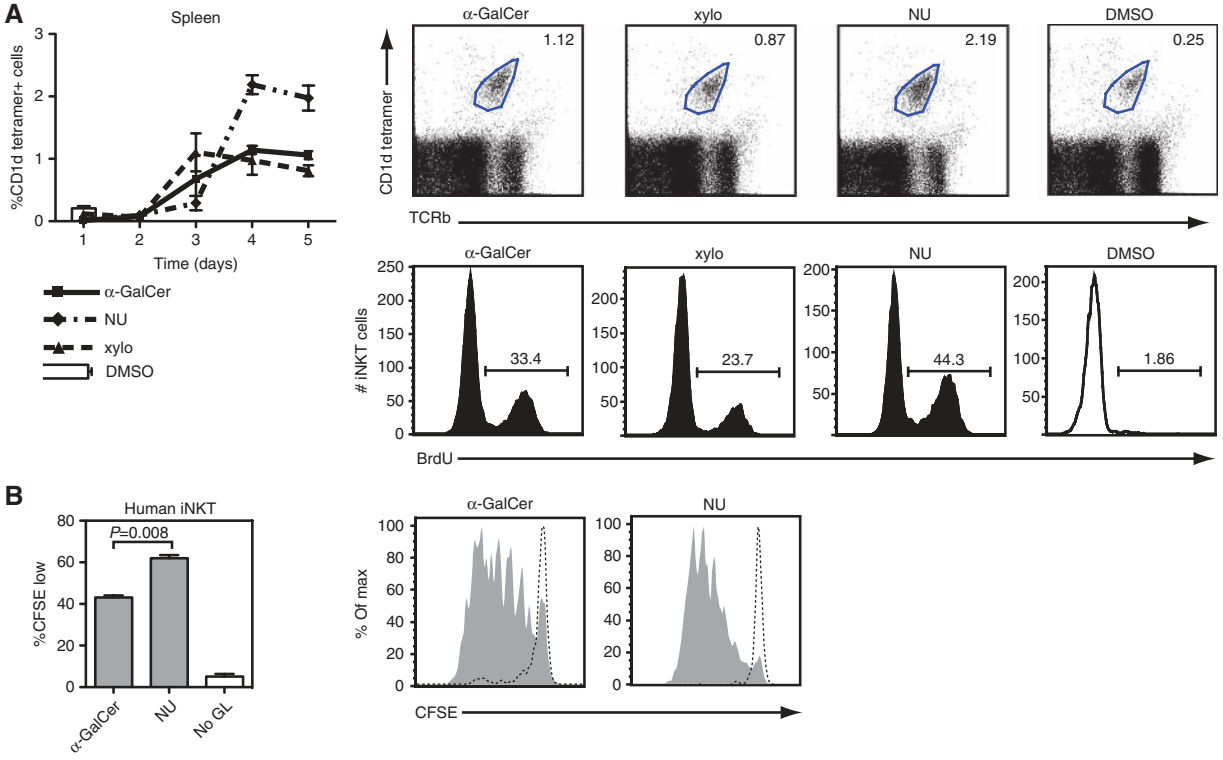

Figure 3 Glycolipid-pulsed bone marrow dendritic cells (BMDCs) induce iNKT cell expansion. (**A**) Spleen iNKT cells ($TCRb_{intermediate}$, CD1d–α-GalCer tetramer-positive cells) were stained 1, 2, 3, 4 and 5 days after adoptive transfer of 600 000 glycolipid-loaded BMDCs. Animals were injected intraperitoneally with BrdU 16 h before they were sacrificed. Dot plots and histograms of iNKT cells show a marked increase in expansion and proliferation (as measured by BrdU uptake) 5 days after injection of NU-α-GalCer-loaded BMDCs compared with α-GalCer. At each time point, 3 mice/group were analysed. Data are representative of two independent experiments. (**B**) Proliferation of human iNKT cells after co-culture with glycolipid-loaded PBMCs. Human iNKT cells (10^4) from five healthy individuals were labelled with CFSE (1 μM) and stimulated with α-GalCer, NU-α-GalCer or DMSO-loaded irradiated autologous PBMC (10^5), in the presence of IL-2 (0.1 U/ml). At day 7, cells were harvested and labelled with 6B11 (Ab recognizing the human invariant Vα24Jα18-CDR3 loop) and 7-AAD to gate out dead cells. CFSE dilution of iNKT cells (6B11 +) was measured by flow cytometry. Similarly as for mice, NU-α-GalCer induces an increased expansion of human iNKT cells as observed by the stronger CFSE dilution compared with α-GalCer. Data are shown as mean percentage of CFSE diluted cells (with s.e.m.). Graphs shown are representative for one out of five independent experiments.

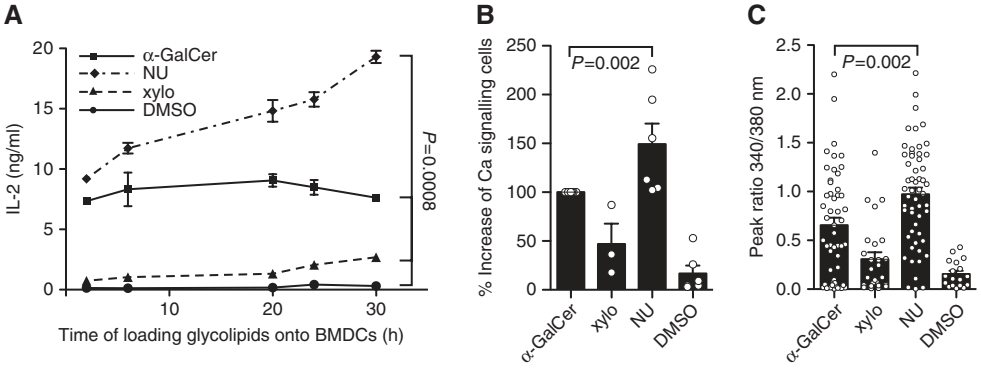

Figure 4 NU-α-GalCer induces a stronger iNKT cell response when bound to bone marrow-derived dendritic cells (BMDCs). BMDCs were grown with GM-CSF for 10 days and subsequently loaded with a glycolipid (100 ng/ml) for 2 h. (**A**) Co-culture with an iNKT cell line (2C12) was set up for 16 h and IL-2 production was measured by ELISA. Xylo-α-GalCer, NU-α-GalCer and DMSO significantly differ from α-GalCer (two-tailed Mann–Whitney *U*-test). Data are shown as mean with s.e.m. ($n = 5$). One representative experiment of two independent experiments. (**B**) The iNKT cell line (2C12) was loaded with FURA-2 and added to glycolipid-pulsed BMDCs. Five minutes later, calcium signals in iNKT cells were measured using epifluorescence microscopy. On average, about 50 cells were monitored for 10 min. An increase of fluorescence of about 10% was determined as a cell displaying an increase in intracellular calcium concentration. The percentage of increase was normalized to 100% for α-GalCer. NU-α-GalCer induced more cells to increase their calcium concentration. Representation of pooled data from four independent experiments. (**C**) Peak value of transient calcium changes expressed as ratiometric FURA-2 measurements. NU-α-GalCer displays higher increases in calcium concentration compared with α-GalCer. Every dot represents a cell displaying a calcium transient. Data are shown as mean with s.e.m. Four similar experiments were performed.

it has a weaker profile as it induces both less IL-4 and IFN-γ compared with NU-α-GalCer (Supplementary Figure S4).

Biochemical characterizations

We measured the equilibrium binding constants of the refolded Vα14Vβ8.2 TCR towards the α-GalCer analogues

NU-α-GalCer, α-C-GalCer and BnNH-GSL-1′ bound to mouse CD1d by SPR (Supplementary Figure S1). With an equilibrium binding constant (K_D) of 39.6 nM, the TCR-binding affinity towards NU-α-GalCer is slightly weaker than to α-GalCer (11.2 nM) (Wang *et al*, 2010), while both BnNH-GSL-1′ and α-C-GalCer are much weaker than α-GalCer (K_D of 187 and 247 nM, respectively) but higher in affinity than the bacterial antigen GalA-GSL aka GSL-1′ ($K_D = 0.7\,\mu M$) (Wang *et al*, 2010). The kinetic parameters reveal that the TCR binds all four glycolipids with a similar association rate (k_a between 0.98×10^5 and 1.18×10^5/M per second). However, the dissociation of NU-α-GalCer is slightly faster than α-GalCer (2–3 times) ($k_d = 3.8 \times 10^{-3}$ per second), while both BnNH-GSL-1′ and α-C-GalCer dissociate 15–20 times faster ($k_d = 2.2 \times 10^{-2}$ and 2.83×10^{-2} per second, respectively) than α-GalCer ($k_a = 1.3 \times 10^5$/M per second and $k_d = 1.45 \times 10^{-3}$ per second) (Wang *et al*, 2010). In summary, the kinetic data indicate that the initial binding of the TCR to all four mCD1d–glycolipids complexes is very similar. This suggests that their binding to CD1d before TCR engagement is similar, in contrast to microbial antigens that bind differently to mCD1d before TCR engagement and, therefore, have a different TCR association rate (Li *et al*, 2010). As a result, the chemical differences between the analysed glycolipids are mostly affecting the dissociation rate, and thus the stability of the CD1d–glycolipid–TCR complexes.

Crystal structures of the TCR complexes

To elucidate the structural details of the mCD1d–NU-α-GalCer–TCR interaction and to understand how the relatively large 6″-naphthylurea substituent can be accommodated between the mCD1d–TCR interface without a significant reduction in TCR-binding affinity, we crystallized the TCR–NU-α-GalCer–mCD1d complex and determined the structure to 2.3 Å resolution (Figure 5; Supplementary Table S1). For comparison, we have also determined the crystal structures of the mCD1d–α-C-GalCer–TCR complex, as well as the

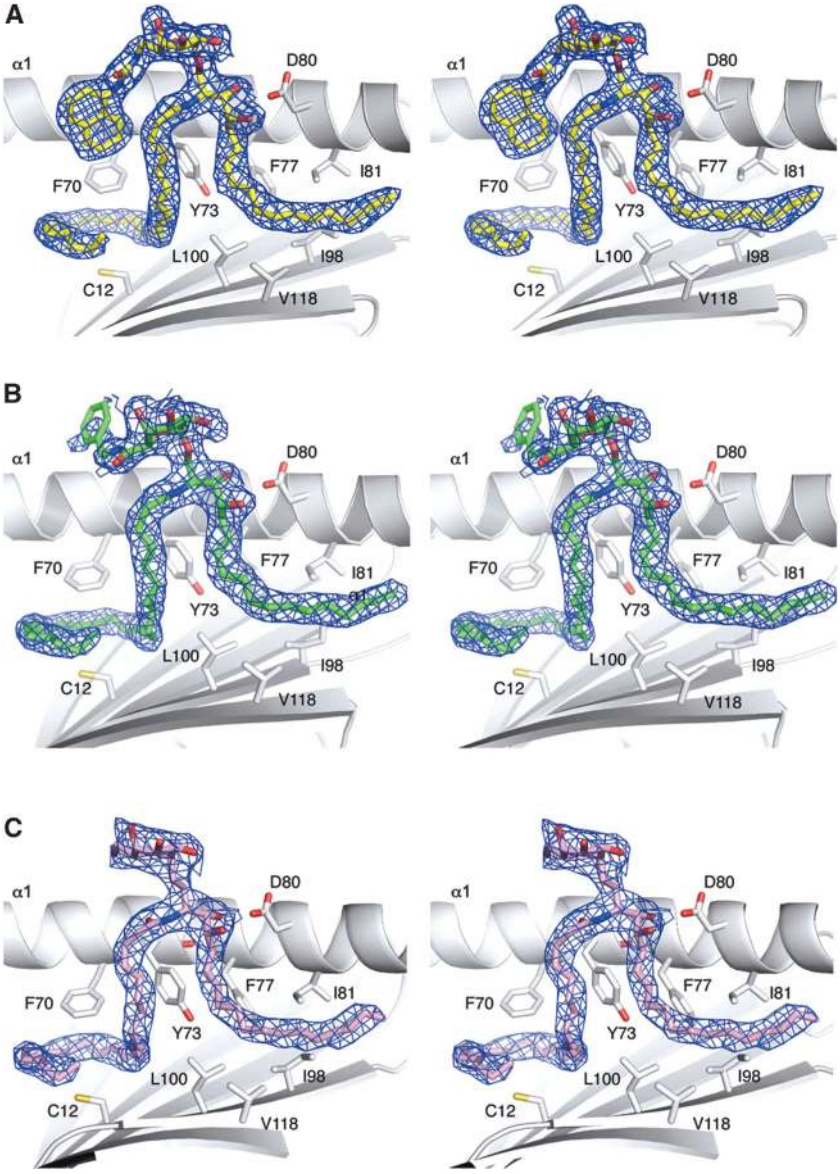

Figure 5 Stereoview of the electron density for the different mCD1d-bound glycolipids. The 2Fo-Fc electron density map is contoured at 1σ and shown as a blue mesh around the glycolipid ligands NU-α-GalCer (**A**), BnNH-GSL-1′ (**B**) and α-C-GalCer (**C**) in a side view. Several hydrophobic mCD1d residues interacting with the lipids are depicted. Note that the electron density for the phenyl moiety of BnNH-GSL-1′ that is exposed into the solvent is rather poor, indicating a slight disorder, which stems from lack of defined contacts with either CD1d or TCR residues.

mCD1d–BnNH-GSL-1′–TCR complex to 2.9 and 2.25 Å, respectively. Each structure contains one ternary complex in the asymmetric unit of the crystal and exhibited very clear electron density for each of the glycolipid ligands after molecular replacement, which allowed for unambiguous fitting of the glycolipid ligand (Figure 5).

Similar to α-GalCer, all three glycolipids are bound with their phytosphingosine chain inserted in the F′ pocket and the long-chain fatty acid in the A′ pocket, where it encircles the A′ pole (Cys12–Phe70) in the typical anti-clockwise orientation, when looked upon from the top of the binding. The α-linked galactose moieties are similarly exposed at the CD1d binding grooves for TCR recognition. Strikingly, the 6″-naphthyl ring that distinguished NU-α-GalCer from α-GalCer sits above the A′ pole, but faces down into a small binding pocket formed by induced fit (see later), rather than being exposed into the solvent, where it could interfere with TCR binding.

TCR docking and ligand recognition

Overall, the TCR adopts a docking mode nearly identical to the recently determined TCR–α-GalCer–mCD1d complex directly above the F′ pocket of mouse CD1d (Figure 6A; Supplementary Figure S5; Pellicci *et al*, 2009). In all ternary complex structures, TCR contacts with mCD1d are dominated mainly by the CDR2β and CDR3α loop, similar as observed in the TCR–α-GalCer–mCD1d complex. However, due to the usage of a different CDR3β rearrangement (CASGDEGYTQYF), which results in a 3-amino acid shorter CDR3β loop compared with the Vα14Vβ8.2 TCR used in the α-GalCer complex (CASGDAGGNYAEQFF), additional contacts are formed between CDR3β and mCD1d in the NU-α-GalCer, α-C-GalCer and BnNH-GSL-1′ complex structures (Supplementary Figure S5). CDR3β, which is disordered in the ternary structure of the TCR–α-GalCer–mCD1d complex (Pellicci *et al*, 2009), is well ordered in our three structures and exclusively forms both van der Waals interactions, as well as one salt bridge interaction through Asp96β with Lys148 on the α2 helix of mCD1d (the latter only for NU-α-GalCer and BnNH-GSL-1′) (Supplementary Figure S5). The galactose moiety of each glycolipid is exposed for recognition by the TCR. The contacts between the TCR and NU-α-GalCer are exactly the same as those observed between the TCR and α-GalCer. Specifically, the 2″-OH group of the galactose ring forms an H-bond with Gly96 of CDR3α and the 3″- and 4″-OH groups of the galactose form H-bonds with Asn30 of CDR1α loops of TCR. The 3-OH of the sphingosine chain also form hydrogen bonds to Arg95α of CDR3α (Figure 6B). However, both BnNH-GSL-1′ and α-C-GalCer form only three instead of four H-bonds with the TCR. In BnNH-GSL-1′, the galactose is tilted slightly downward into the CD1d groove, moving the 4″-OH of the galactose away from the Asn30α. α-C-GalCer loses an H-bond between R95α of the TCR and the 3-OH of the phytophingosine chain, due to a slight rotation of the ceramide backbone. As a consequence, the TCR interaction with NU-α-GalCer is comparable to α-GalCer, while both BnNH-GSL-1′ and α-C-GalCer form less stable interactions, which is in agreement with the observed increase in TCR dissociation rates.

Ligand binding and induced fit in CD1d

Binding of NU-α-GalCer to mCD1d parallels that of α-GalCer. All hydrogen bond interactions that were described for

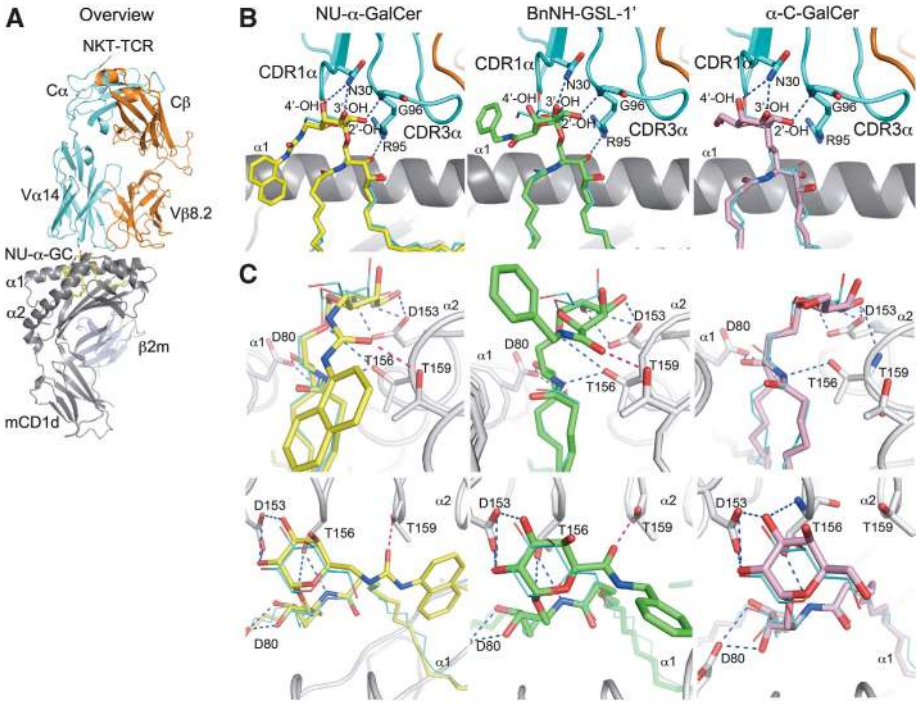

Figure 6 Binding comparison of NU-α-GalCer, BnNH-GSL-1′ and α-C-GalCer with α-GalCer. (**A**) Overview of the mCD1d–NU-α-GalCer–Vα14Vβ8.2 TCR ternary complex. (**B**) Binding of the TCR (cyan) to the glycolipids NU-α-GalCer (yellow), BnNH-GSL-1′ (green) and α-C-GalCer (salmon), which are superimposed onto α-GalCer (thin cyan sticks, from PDB ID 3HE6) for comparison. Hydrogen bond interactions are indicated with blue dashed lines. (**C**) H-bonds between the glycolipids and CD1d are conserved, however, an additional conserved H-bond between the carbonyl oxygen of NU-α-GalCer and BnNH-GSL-1′ with Thr159 of CD1d is formed (red dashed lines), resulting in a tilt of the BnNH-GSL-1′ galactose. Also, α-C-GalCer 3′-OH of galactose forms an additional 3.5 Å H-bond with the backbone amide of Thr156, while losing the glycosidic H-bond (middle row). Bottom row illustrates H-bond interactions between glycolipids and mCD1d from a TCR view.

α-GalCer involving the 2″- and 3″-OH of the galactose and the 3- and 4-OH of the ceramide backbone with CD1d residues Asp80, Asp153 and Thr156, are also conserved in the NU-α-GalCer structure (Figure 6C). In addition, NU-α-GalCer forms an additional H-bond between the carbonyl oxygen of the urea linker that connects the galactose and the naphthyl moieties. Interestingly, the same H-bond is also formed between the carbonyl oxygen of BnNH-GSL-1′, however, as this carbonyl is in closer proximity to the galactose, the formation of that interaction pulls the galactose down towards CD1d and away from the TCR. This results in the aforementioned loss of one H-bond with the TCR (Figure 6B and C). α-C-GalCer cannot form the H-bond between the α-anomeric oxygen and Thr156, as the oxygen is replaced by carbon, instead it forms a novel H-bond between the 2″-OH of galactose with the backbone oxygen of Thr156 (Figure 6C).

The most striking difference between NU-α-GalCer and α-GalCer, BnNH-GSL-1′ or α-C-GalCer is the aforementioned induced fit in CD1d. In order to accommodate the naphthyl group of NU-α-GalCer between the α1 and α2 helices of CD1d both helices are opened laterally by about 1.3 Å. The distance between the backbones of Met69 (α1 helix) and Thr159 (α2 helix) of CD1d is increased from 9.2 to 10.5 Å (Figure 7A). In addition, the side chain of Met69, which is involved in the formation of the A′ roof, adopts a different conformation, thereby creating a narrow hydrophobic cleft formed by Leu66, Met69, Phe70 and Leu163 on top of the A′ roof, in which the aromatic substitution is nicely accommodated (Figure 7B). The binding of the aromatic group in this pocket forms a third anchor in addition to the two more deeply inserted alkyl chains, thus increasing the van der Waals interactions between ligand and CD1d. We have qualitatively assessed the mCD1d–glycolipid stability in a modified SPR assay using an α-GalCer-specific antibody to monitor loss of binding to CD1d due to dissociation of glycolipid from CD1d (Figure 7C). NU-α-GalCer exhibits much more interactions with CD1d (117 vdw and 8 H-bond interactions, 1150 Å^2 interface surface) than with α-GalCer (95 vdw, 7 H-bonds, 1027 Å^2 interface surface) leading to a slightly increased binding affinity of NU-α-GalCer to CD1d as compared with α-GalCer (Supplementary Table S2; Figure 7C). The slightly increased CD1d binding stability of NU-α-GalCer compared with α-GalCer is in general agreement with the roughly 10% increase in both buried surface area and contacts formed between lipid and mCD1d. The NU linker also pulls the galactose slightly down into the groove, similar but far less pronounced than observed for BnNH-GSL-1′. This results in slightly less intimate packing against Pro28 of the TCR CDR1α (not shown) and an increased distance of the H-bond between 4″-OH of NU-α-GalCer and Asn30 of the TCR, which could be the reason for the 2–3 faster TCR dissociation compared with α-GalCer. Thus, NU-α-GalCer induces marked structural changes in CD1d, that are strictly dependent upon the addition of aromatic moiety with judiciously chosen linker length, as shorter linkers result in exposure of the aromatic ring into the solvent, as seen for BnNH-GSL-1′.

Discussion

Our results provide new insights into the mechanisms controlling TCR responses to glycolipids by showing that addition of aromatic groups at the galactose part of α-GalCer can lead to an additional binding pocket of mCD1d through an induced fit mechanism. This in turn slightly enhances the affinity of the glycolipids for CD1d leading to a more sustained interaction with the iNKT TCR and lowers thresholds for iNKT cell activation. This is accompanied by skewed

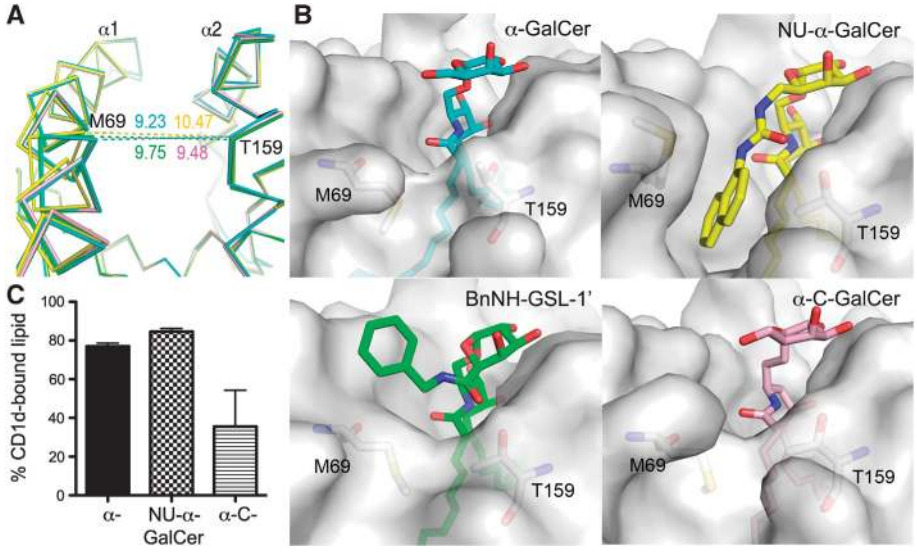

Figure 7 Induced fit in mCD1d upon NU-α-GalCer binding. (**A**) Superposition of the α1 and α2 helix backbones of CD1d in the four ternary structures. α-GalCer, cyan; NU-α-GalCer, yellow; BnNH-GSL-1′, green and α-C-GalCer, salmon. The distances between the backbones of Met 69 (M69) and Thr 159 (T159) of CD1d are indicated in Å and colour-coded accordingly. Note that binding of NU-α-GalCer results in an induced fit that widens the binding groove laterally by >1.2 Å to accommodate the naphthyl group. (**B**) Surface representation of mouse CD1d binding grooves with bound lipid ligands coloured as in (**A**). The alternate conformation of Met 69 forms a small pocket on top of the A′ roof that accommodates the aromatic group of the NU-α-GalCer ligand. (**C**) CD1d–glycolipid stability assay. The dissociation of glycolipids from CD1d under constant flow of running buffer was monitored after 18 h. Note that under these conditions, slightly more NU-α-GalCer remains bound to CD1d compared with α-GalCer, indicating increased CD1d–lipid stability, while α-C-GalCer dissociates much faster from mCD1d. The experiment was performed twice and also carried out using 0.5% Tween-20 (not shown), which indicated a similar trend.

cytokine patterns, providing an additional and previously unappreciated mode of modulating iNKT cell responses. This is in sharp contrast to MHC I or II binding where no formation of additional pockets has been reported upon peptide binding, although there is a dynamic interaction between peptide and MHC that can affect the conformation of the α2 helix at the position where it forms the typical kink (Borbulevych *et al*, 2009). Additionally, previous studies on conformational changes of CD1d are scarce and limited to the F′ pocket. It was shown previously that binding of α-GalCer to CD1d results in an induced fit above the F′ pocket, leading to the formation of the F′ roof. To date, α-GalCer is the only lipid that can form the F′ roof before TCR binding, while in two previously determined complex structures with microbial antigens the F′ roof is formed only after TCR binding, likely through the hydrophobic finger L99 of TCR CDR3α′ (Li *et al*, 2010). We previously proposed the formation of the F′ roof to be a key determinant in modulating the TCR affinity, especially the TCR off-rate (Li *et al*, 2010). Earlier studies proposed that the F′ pocket could also partially collapse when containing short-chain lipids, such as OCH (McCarthy *et al*, 2007), which would alter the F′ roof and change the TCR recognition surface. However, both the mCD1d–OCH binary structure as well as the more recent mCD1d–OCH–TCR ternary structure (Wun *et al*, 2011) do not reveal such gross structural changes because of the presence of a spacer molecule in the remainder of the F′ pocket (Sullivan *et al*, 2010). Thus, the ability to form the F′ roof is important in modulating TCR affinities, with highest affinities for those ligands that can pre-form the F′ roof upon binding to CD1d, while a partial collapse of the F′ pocket when shorter lipids are bound is unlikely. Conformational changes induced by modifying the sugar part of the glycolipid, however, are not yet known, nor has a major induced fit been seen upon glycolipid binding for any other region of CD1d besides the F′ pocket, nor any other ligand besides α-GalCer or possibly its analogues. Thus, our study reveals a previously unappreciated flexibility of CD1d that can be further exploited for the design of synthetic glycolipid ligands that enhance the binding affinity towards CD1d without disrupting the TCR-binding interface.

Efficient iNKT cell activation is requisite for providing subsequent anti-tumour immunity. This is exemplified by the key roles assigned to Th1-polarizing cytokines such as IFN-γ and IL-12 produced by dendritic cells, macrophages and NK cells that arise downstream of iNKT cell activation (Wesley *et al*, 2005). Most of the current studies involving Th1-polarizing glycolipids focus on α-C-GalCer (Schmieg *et al*, 2003; Fujii *et al*, 2006), which features a stabilized glycosidic bond. By contrast, here we report on the physiological effects of a group of strong Th1-polarizing analogues characterized by alterations at the 6′-position of the galactose. In contrast to what is observed for the α-C-GalCer, both the expansion of the iNKT cell pool and cytokine production in response to these glycolipids were very conserved between men and mice. Additionally when loaded on BMDCs NU-α-GalCer was markedly more potent than α-GalCer in preventing the growth of B16 tumours. Although several types of structural modification of the galactose moiety of α-GalCer may lead to Th1 bias, this is generally at the expense of the overall antigenic potency. Strikingly, the absolute cytokine levels for IFN-γ and IL-12 achieved by NU-α-GalCer *in vivo* seem to equal or surpass the levels measured by α-GalCer, yet Th2 cytokines are markedly lower. Although it has been suggested that loading of Th1-polarizing analogues onto CD1d occurs primarily within endosomal compartments (Bai *et al*, 2009; Im *et al*, 2009), APC lacking the cytoplasmic tail of CD1d (therefore, they are not able to load endosomal glycolipids onto CD1d) was able to present NU-α-GalCer (data not shown), suggesting there may be an alternate mechanism for the observed Th1 polarization.

To understand the structural basis of observed functional differences, X-ray crystallographic studies were undertaken in which α-C-GalCer and NU-α-GalCer were compared with α-GalCer. Surprisingly, NU-α-GalCer showed much more interaction with CD1d than with α-GalCer, which is primarily caused by formation of an induced fit above the A′ pocket between Met69 and Thr159. The resulting hydrophobic pocket is perfectly suited in both shape and hydrophobicity to bind the naphthyl group of NU-α-GalCer as a third anchor, in addition to the A′ and F′ pockets. The importance of the pocket formation in the strong Th1 polarization was further substantiated by the crystal structure with BnNH-GSL-1′, a weaker Th1-polarizing analogue, which exhibits a shorter linker to the phenyl ring and bears the carbonyl group immediately next to the sugar ring instead of two bonds further as in NU-α-GalCer. Both carbonyl atoms form an extra H-bond to Thr159 from the α2 helix of CD1d. However, the H-bond of BnNH-GSL-1′ leads to a noticeable tilt of the galactose due to the shorter linker and, hence, reduced TCR affinity. NU-α-GalCer recapitulates both an optimal overall linker length to induce the formation of the third small anchor pocket, as well as the correct spacing between the carbonyl oxygen and the galactose to form the conserved H-bond with Thr159 without significantly affecting the galactose orientation. Thus, a conceptual new model has arisen in which additional aromatic groups can interact with CD1d.

Structural changes have so far only been observed around the F′ pocket (Li *et al*, 2010) of CD1d where they enhance the surface area that is contacting the TCR. In the case of NU-α-GalCer, the induced fit above the A′ pocket results in increased hydrophobic interactions between glycolipid NU-α-GalCer and CD1d, which, together with the additional hydrogen bond, likely enhance the stability and half-life of the CD1d–NU-α-GalCer complex. The widening of the helices and the alternate side chain conformation of Met69 suggests that the CD1d binding groove has the potential to structurally adapt to accommodate different functional groups of α-GalCer derivatives. Thus, although no CD1d polymorphisms have been described, our results illustrate the existence of another mechanism to accommodate distinct antigens. However, as the TCR–BnNH-GSL-1′–mCD1d structure reveals, those modifications have to be connected to the galactose with a judiciously chosen linker length, since shorter linkers likely result in exposure of the aromatic ring into the solvent. This new mode of structural modification of CD1d therefore broadens the spectrum of glycolipids that can stimulate iNKT cells and may facilitate the design of a new spectrum of glycolipid antigens to bind and stimulate iNKT cells. This highlights a delicate balance between the structure–function relationship of CD1d–glycolipid–iNKT TCR complex.

Despite its well-recognized Th1-biasing profile, α-C-GalCer differs substantially from NU-α-GalCer by a number of biochemical and structural properties. Despite a similar initial

binding of the TCR, the dissociation rate, and thus the stability of the CD1d–glycolipid–TCR complexes is markedly lower. This is in line with an earlier reported weak TCR stimulus. The underlying structural basis has been unveiled here by the crystallographic structure, which showed that α-C-GalCer forms only three instead of four H-bonds with the TCR. In addition, α-C-GalCer cannot form the H-bond between the α-anomeric oxygen and Thr156, as the oxygen is replaced by carbon, instead it forms a novel H-bond between the 2″-OH of galactose with the backbone oxygen of Thr156. Even though the interaction between α-C-GalCer, CD1d and iNKT TCR are weaker than α-GalCer, it is characterized by long-lived, functional complexes on the surfaces of APCs *in vivo* (Sullivan *et al*, 2010). In this context, it should be highlighted that the C-glycoside variant of α-GalCer was designed to provide additional biochemical stability in order to prevent degradation by O-glycosidase enzymes. This may result in increased stability of a cell-associated pool of α-C-GalCer and as such allow continuous replenishment of cell surface complexes. Thus, distinct modes of modifying the interaction between CD1d–glycolipid–iNKT TCR complex exist that affect the functional outcome of glycolipid reactive T cells.

Overall, these findings highlight the previously unexploited flexibility of CD1d in accommodating galactose-modified glycolipids by providing an additional binding pocket of mCD1d through an induced fit mechanism. We speculate that these glycolipids may be useful targets for inducing, superior and more sustained iNKT cell responses *in vivo*. Whether a similar induced fit mechanism is also utilized by microbial antigens including alternate modifications such as additional fatty acids is an interesting question to be explored.

Materials and methods

Synthetic glycolipids

Glycolipids were synthesized in the Laboratory of Medicinal Chemistry (Trappeniers *et al*, 2008) and at the Department of Chemistry, Hunter College/CUNY (Schmieg *et al*, 2003). OCH and α-C-GalCer were kindly provided M Tsuji (Aaron Diamond AIDS Research Center, NY, USA) and the NIH Tetramer Core Facility. Lyophilized glycolipids were dissolved in pure DMSO (Sigma) at 10 mg/ml concentration and stored at −20°C. Glycolipids were solubilized by adding PBS (Invitrogen) or vehicle (96 mg/ml sucrose, 10 mg/ml sodium deoxycholate, 0.05% Tween-20), warming to 80°C for 20 min, sonication for 10 min.

Recombinant protein expression and purification

Mouse CD1d-β2-microglobulin (β_2M) heterodimeric protein was expressed and purified using the baculovirus expression system as reported previously (Zajonc *et al*, 2005b). TCR refolding and purification was carried out as reported previously (Wang *et al*, 2010). Pure TCR was stored in Superdex S200 running buffer (50 mM Hepes, 150 mM NaCl pH 7.4) until further use.

Glycolipid loading and NU-α-GalCer–mCD1d–TCR complex formation

Lipids NU-α-GalCer, BnNH-GSL-1′ and α-C-GalCer were dissolved in DMSO at 1 mg/ml. Before loading, 60 μl of each glycolipid solution was diluted to 0.25 mg/ml with 60 μl vehicle solution (50 mM Tris–HCl pH 7.0, 4.8 mg/ml sucrose, 0.5 mg/ml sodium deoxycholate and 0.022% Tween-20) and 120 μl of 10 mg/ml Tween-20. The diluted glycolipids were heated in a bath at 80°C for 20 min and cooled at room temperature for 5 min. Glycolipids were loaded onto mCD1d by incubating 400 μl mouse CD1d (2.5 mg/ml) overnight with 240 μl pre-heated glycolipid solution (molar ratio of protein to lipid is 1:3) and 800 μl buffer (50 mM Tris–HCl pH 7.0). For CD1d–TCR complex formation, the refolded TCR was incubated at room temperature for 30 min with lipid-loaded mCD1d at a ratio of 1:2 molar ratio for NU-α-GalCer and BnNH-GSL-1′ and 1:3 for α-C-GalCer, as the NU-α-GalCer loading efficiency is only 40–50% (measured using the α-GalCer-specific antibody L317 in a modified SPR experiment) and we expected even lower loading efficiencies for α-C-GalCer. The ternary mCD1d–lipid–TCR complexes were isolated from uncomplexed mCD1d and TCR by size exclusion chromatography using Superdex S200 10/300 GL (GE Healthcare) for crystallization.

SPR studies

SPR studies were conducted using a Biacore 3000 (Biacore) as reported previously (Wang *et al*, 2010). The lipids were loaded to biotinylated birA-tagged mCD1d in the same way as non-birA-tagged mCD1d. In all, 300–500 response units (RU) of mCD1d–glycolipid complexes were immobilized onto a streptavidin sensor chip (Biacore) surface by injection at 5 μl/min (10 mM HEPES, 150 mM NaCl, 3.0 mM EDTA, pH 7.4). A reference surface was generated in another flow channel with unloaded mCD1d immobilized at RU of 500. During the association phase, a series of increasing concentrations of TCR in duplicate were injected for 3 min and the dissociation phase initiated by passage of running buffer alone was continued over 30 min. Experiments were carried out at 25°C with a flow rate of 30 μl/min and performed at least two to three times, each time with a different batch of TCR preparation. Kinetic parameters were calculated after subtracting the response to mCD1d molecules in the reference channel, using a simple Langmuir 1:1 model in the BIA evaluation software version 4.1. One representative sensorgram for each lipid is shown.

CD1d–glycolipid stability assay

The assay was modified from previous work (Sullivan *et al*, 2010) to control for loss of proper folding of mCD1d over the course of the experiment. The lipids α-GalCer, NU-α-GalCer and α-C-GalCer were loaded to biotinylated mCD1d as mentioned above. In all, 1000–2000 RU of each mCD1d–lipid were immobilized on a streptavidin sensor chip (GE Healthcare). A reference surface was generated in another flow channel with unloaded mCD1d immobilized at 1500 RU. The percentage of correctly folded CD1d on the chip at the beginning and at the end of the experiment was measured with a conformation-specific anti-mouse CD1d antibody (clone 1B1, BD Biosciences). The binding of a saturating concentration (1 μM) of the α-GalCer-specific L317 antibody was used to monitor the stability of mCD1d–lipid complexes over time while flowing buffer with a high detergent content (10 mM HEPES, 150 mM NaCl, 3.0 mM EDTA, pH 7.4, 0.2% Tween-20, 30 μl/min) to assist extraction of the lipid from the CD1d binding groove. Binding responses after 18 h were normalized against the initial RU reading and corrected for the amount of folded CD1d still present on the surface, as measured with the 1B1 antibody.

Crystallization and structure determination

Detailed methods are available in the online supplementary material.

Cell lines

The murine iNKT hybridoma N38-2C12 (Vα14Vβ8.1/8.2*b*) was provided by L Brossay (Burdin *et al*, 1998) (Brown University, Providence, RI, USA). Cells were cultured in DMEM (Sigma) supplemented with 10% fetal calf serum (Invitrogen), 1% glutamin (Sigma), 1% penicillin streptomycin (Sigma) and 2-mercaptoethanol (Sigma) (called cDMEM hereafter).

Isolation and expansion of BMDCs

BMDCs were isolated from the mouse bone marrow as described previously (Lutz *et al*, 1999).

Mice

C57BL/6 mice were in house bred (in accordance with the general recommendations for animal breeding and housing) or purchased from the Harlan Laboratory, Jα18-knockout and CD1d-knockout mice on the C57BL/6 background were kindly provided by M Taniguchi (Cui *et al*, 1997) (RIKEN, Tsurumi, Yokohama, Japan) and L Van Kaer (Mendiratta *et al*, 1997) (Vanderbilt University School of Medicine, Nashville, TN, USA), respectively. Experiments were conducted according to the guidelines of the Ethical Committee

of Laboratory Animals Welfare of Ghent University. Mice used for experiments were between 5 and 12 weeks old.

In vitro and in vivo activation of iNKT cells

For *in vitro* stimulation, murine iNKT hybridoma cells at 5.10E4 cells/well in 96-well plates were stimulated with the 10E5 cells/well glycolipid-pulsed BMDCs in cDMEM for 16 h at 37°C, and levels of murine IL-2 secretion were determined by ELISA.

For *in vivo* activation of iNKT cells, C57BL/6 mice were either intraperitoneally injected with 5 μg glycolipid (dissolved in PBS) or intravenously with 6.10E5 or 1.10E4 glycolipid-pulsed BMDCs.

Calcium level analysis in iNKT hybridoma

2C12 cells were loaded with the calcium-sensitive probe Fura-2 AM (15 μM) (Sigma) for 1 h at 37°C in PBS in the presence of pluronic acid (1.5 μl) (Molecular Probes), followed by 30 min deesterification at room temperature and added to glycolipid-pulsed BMDCs (1.4×10E6 cells/ml), grown on 35 mm glass bottom culture dishes (MatTek). Five minutes after start co-culture cytoplasmic-free calcium was monitored with epifluorescence microscopy and digital imaging. Cells were viewed with an inverted epifluorescence microscope (Nikon Eclipse TE300, Analis, Ghent, Belgium) using a $\times 40$ oil immersion lens (CFI Plan Fluor, Nikon) as previously described (De Vuyst *et al*, 2009).

Isolation of human PBMCs and iNKT cells

PBMCs from healthy adult individuals ($n = 5$) were isolated by Ficoll density centrifugation (Histopaque, Sigma diagnostics). PBMC was pre-treated with FcR Blocking Reagent (Miltenyi Biotec) for 10 min before incubation with fluorochrome-conjugated mAbs directed against human TCRVα24 (clone C15-PE) and TCRVβ11 (clone C21-FITC) and 7-AAD (all from BD) for 30 min. Subsequently, Vα24 + Vβ11 + 7-AAD- cells were single cell sorted in 96-well plates using a FACSAria II (BD). iNKT cells were cultured in the presence of irradiated autologous PBMC (10E5), pre-loaded with glycolipids for 18 h, in RPMI 1640 media supplemented with 10% fetal bovine serum, 1% sodium pyruvate, 1% non-essential amino acids and 1% penicillin/streptomycin (all from Invitrogen) containing 5 U/ml IL-2 (Roche).

For proliferation assays, 10E4 iNKT cells were labelled with CFSE (1 μM) and stimulated with glycolipid-loaded irradiated autologous PBMC (10E5), in the presence of IL-2 (0.1 U/ml). At day 7, cells were harvested and labelled with 6B11 (eBioscience) and 7-AAD to gate out dead cells. CFSE dilution was measured by flow cytometry. Supernatants were collected and used for cytokine measurements by ELISA or CBA assays.

Isolation of murine lymphocytes

Spleen and liver cells were isolated as previously described (Franki *et al*, 2006). Lymphocytes were isolated at the interface and washed and resuspended in staining buffer containing saturating amount of anti-Fcγ Receptor type II/type III monoclonal antibodies (Miltenyi Biotec, Sunnyvale, CA). PE-labelled CD1d/α-GalCer tetramers were added at room temperature, 15 min before the addition of TCRb (H57-597, eFluor 780, eBioscience) during 30 min on ice. For proliferation analysis, cells were fixed, permeabilized and incubated with DNAse (Sigma) and stained with anti-BrdU (BD). Live cells were acquired on a FACSCanto (BD) flow cytometer and analysed using FlowJo (Tree Star) software.

Statistical analysis

The statistical test used throughout this study was Kruskal–Wallis test with Dunn's multiple comparison test or Mann–Whitney *U*-test (unpaired, two-sided). Data were analysed using Excel (Microsoft) and Graphpad Prism 5.

Supplementary data

Supplementary data are available at *The EMBO Journal* Online (http://www.embojournal.org).

Acknowledgements

Julie Coudenys and Evelyne Verheugen for ELISA; Kim Deswarte for FACS Sort; Luc Van Kaer for CD1d−/− mice; Taniguchi for Ja18−/− mice; Moria Tsuiji and the NIH Tetramer Core facility for providing α-C-GalCer and OCH; Nan Wang for help with calcium experiments; Laurent Brossay and Cindy Banh for useful discussion; Stijn Lambrecht and Lode Melis for help with statistical analysis. Steven A Porcelli for the CD1d-α-GalCer-specific hybridoma line L317. Stanford Synchrotron Radiation Lightsource (SSRL) beamlines 9-2 and 7-1 for remote data collection. DMZ is recipient of an Investigator award from the Cancer Research Institute and supported by NIH grant RO1 AI074952. AS, KVB, KV and MT are supported by FWO Flanders. MD is supported by FWO Flanders and is a member of Group-ID consortium. DE and SVC received support of the Belgian Stichting tegen Kanker and the FWO Flanders.

Author contributions: AS, YL, EDY, TD, KVB, KV, EG, JW, DMZ and DE performed and designed most experiments; AS, KVB, YL, EDY, EG, KV, MD, DMZ and DE analysed the data; LL designed calcium experiments, RF, MT, NP and SVC synthesized the glycolipids; and AS, YL, DMZ and DE wrote the manuscript.

Conflict of interest

The authors declare that they have no conflict of interest.

References

Airoldi I, Di Carlo E, Cocco C, Taverniti G, D'Antuono T, Ognio E, Watanabe M, Ribatti D, Pistoia V (2007) Endogenous IL-12 triggers an antiangiogenic program in melanoma cells. *Proc Natl Acad Sci USA* **104:** 3996–4001

Bai L, Sagiv Y, Liu Y, Freigang S, Yu KO, Teyton L, Porcelli SA, Savage PB, Bendelac A (2009) Lysosomal recycling terminates CD1d-mediated presentation of short and polyunsaturated variants of the NKT cell lipid antigen alphaGalCer. *Proc Natl Acad Sci USA* **106:** 10254–10259

Borbulevych OY, Piepenbrink KH, Gloor BE, Scott DR, Sommese RF, Cole DK, Sewell AK, Baker BM (2009) T cell receptor cross-reactivity directed by antigen-dependent tuning of peptide-MHC molecular flexibility. *Immunity* **31:** 885–896

Borg NA, Wun KS, Kjer-Nielsen L, Wilce MC, Pellicci DG, Koh R, Besra GS, Bharadwaj M, Godfrey DI, McCluskey J, Rossjohn J (2007) CD1d-lipid-antigen recognition by the semi-invariant NKT T-cell receptor. *Nature* **448:** 44–49

Burdin N, Brossay L, Koezuka Y, Smiley ST, Grusby MJ, Gui M, Taniguchi M, Hayakawa K, Kronenberg M (1998) Selective ability of mouse CD1 to present glycolipids: alpha-galactosylceramide specifically stimulates V alpha 14+ NK T lymphocytes. *J Immunol* **161:** 3271–3281

Chiba A, Oki S, Miyamoto K, Hashimoto H, Yamamura T, Miyake S (2004) Suppression of collagen-induced arthritis by natural killer T cell activation with OCH, a sphingosine-truncated analog of alpha-galactosylceramide. *Arthritis Rheum* **50:** 305–313

Coquet JM, Chakravarti S, Kyparissoudis K, McNab FW, Pitt LA, McKenzie BS, Berzins SP, Smyth MJ, Godfrey DI (2008) Diverse cytokine production by NKT cell subsets and identification of an IL-17-producing CD4-NK1.1-NKT cell population. *Proc Natl Acad Sci USA* **105:** 11287–11292

Cui J, Shin T, Kawano T, Sato H, Kondo E, Toura I, Kaneko Y, Koseki H, Kanno M, Taniguchi M (1997) Requirement for Valpha14 NKT cells in IL-12-mediated rejection of tumors. *Science* **278:** 1623–1626

De Vuyst E, Wang N, Decrock E, De Bock M, Vinken M, Van Moorhem M, Lai C, Culot M, Rogiers V, Cecchelli R, Naus CC, Evans WH, Leybaert L (2009) Ca(2+) regulation of connexin 43 hemichannels in C6 glioma and glial cells. *Cell Calcium* **46:** 176–187

Franki AS, Van Beneden K, Dewint P, Hammond KJ, Lambrecht S, Leclercq G, Kronenberg M, Deforce D, Elewaut D (2006) A unique lymphotoxin \{alpha\}beta-dependent pathway regulates thymic emigr. *Proc Natl Acad Sci USA* **103:** 9160–9165

Fujii S, Shimizu K, Hemmi H, Fukui M, Bonito AJ, Chen G, Franck RW, Tsuji M, Steinman RM (2006) Glycolipid alpha-C-galactosylceramide is a distinct inducer of dendritic cell function during innate and adaptive immune responses of mice. *Proc Natl Acad Sci USA* **103:** 11252–11257

Fujii S, Shimizu K, Kronenberg M, Steinman RM (2002) Prolonged IFN-gamma-producing NKT response induced with alpha-galactosylceramide-loaded DCs. *Nat Immunol* **3:** 867–874

Godfrey DI, MacDonald HR, Kronenberg M, Smyth MJ, Van Kaer L (2004) NKT cells: what's in a name? *Nat Rev Immunol* **4:** 231–237

Im JS, Arora P, Bricard G, Molano A, Venkataswamy MM, Baine I, Jerud ES, Goldberg MF, Baena A, Yu KO, Ndonye RM, Howell AR, Yuan W, Cresswell P, Chang YT, Illarionov PA, Besra GS, Porcelli SA (2009) Kinetics and cellular site of glycolipid loading control the outcome of natural killer T cell activation. *Immunity* **30:** 888–898

Kakuta S, Tagawa Y, Shibata S, Nanno M, Iwakura Y (2002) Inhibition of B16 melanoma experimental metastasis by interferon-gamma through direct inhibition of cell proliferation and activation of antitumour host mechanisms. *Immunology* **105:** 92–100

Kim S, Iizuka K, Aguila HL, Weissman IL, Yokoyama WM (2000) *In vivo* natural killer cell activities revealed by natural killer cell-deficient mice. *Proc Natl Acad Sci USA* **97:** 2731–2736

Kinjo Y, Wu D, Kim G, Xing GW, Poles MA, Ho DD, Tsuji M, Kawahara K, Wong CH, Kronenberg M (2005) Recognition of bacterial glycosphingolipids by natural killer T cells. *Nature* **434:** 520–525

Kitamura H, Iwakabe K, Yahata T, Nishimura S, Ohta A, Ohmi Y, Sato M, Takeda K, Okumura K, Van Kaer L, Kawano T, Taniguchi M, Nishimura T (1999) The natural killer T (NKT) cell ligand alpha-galactosylceramide demonstrates its immunopotentiating effect by inducing interleukin (IL)-12 production by dendritic cells and IL-12 receptor expression on NKT cells. *J Exp Med* **189:** 1121–1128

Koch M, Stronge VS, Shepherd D, Gadola SD, Mathew B, Ritter G, Fersht AR, Besra GS, Schmidt RR, Jones EY, Cerundolo V (2005) The crystal structure of human CD1d with and without alpha-galactosylceramide. *Nat Immunol* **6:** 819–826

Li Y, Girardi E, Wang J, Yu ED, Painter GF, Kronenberg M, Zajonc DM (2010) The Valpha14 invariant natural killer T cell TCR forces microbial glycolipids and CD1d into a conserved binding mode. *J Exp Med* **207:** 2383–2393

Lutz MB, Kukutsch N, Ogilvie AL, Rossner S, Koch F, Romani N, Schuler G (1999) An advanced culture method for generating large quantities of highly pure dendritic cells from mouse bone marrow. *J Immunol Methods* **223:** 77–92

McCarthy C, Shepherd D, Fleire S, Stronge VS, Koch M, Illarionov PA, Bossi G, Salio M, Denkberg G, Reddington F, Tarlton A, Reddy BG, Schmidt RR, Reiter Y, Griffiths GM, van der Merwe PA, Besra GS, Jones EY, Batista FD, Cerundolo V (2007) The length of lipids bound to human CD1d molecules modulates the affinity of NKT cell TCR and the threshold of NKT cell activation. *J Exp Med* **204:** 1131–1144

Mendiratta SK, Martin WD, Hong S, Boesteanu A, Joyce S, Van Kaer L (1997) CD1d1 mutant mice are deficient in natural T cells that promptly produce IL-4. *Immunity* **6:** 469–477

Miyamoto K, Miyake S, Yamamura T (2001) A synthetic glycolipid prevents autoimmune encephalomyelitis by inducing TH2 bias of natural killer T cells. *Nature* **413:** 531–534

Pellicci DG, Patel O, Kjer-Nielsen L, Pang SS, Sullivan LC, Kyparissoudis K, Brooks AG, Reid HH, Gras S, Lucet IS, Koh R, Smyth MJ, Mallevaey T, Matsuda JL, Gapin L, McCluskey J, Godfrey DI, Rossjohn J (2009) Differential recognition of CD1d-alpha-galactosyl ceramide by the V beta 8.2 and V beta 7 semi-invariant NKT T cell receptors. *Immunity* **31:** 47–59

Schmieg J, Yang G, Franck RW, Tsuji M (2003) Superior protection against malaria and melanoma metastases by a C-glycoside analogue of the natural killer T cell ligand alpha-galactosylceramide. *J Exp Med* **198:** 1631–1641

Sullivan BA, Nagarajan NA, Wingender G, Wang J, Scott I, Tsuji M, Franck RW, Porcelli SA, Zajonc DM, Kronenberg M (2010) Mechanisms for glycolipid antigen-driven cytokine polarization by Valpha14i NKT cells. *J Immunol* **184:** 141–153

Trappeniers M, Van Beneden K, Decruy T, Hillaert U, Linclau B, Elewaut D, Van Calenbergh S (2008) 6′-derivatised alpha-GalCer analogues capable of inducing strong CD1d-mediated Th1-biased NKT cell responses in mice. *J Am Chem Soc* **130:** 16468–16469

Wang J, Li Y, Kinjo Y, Mac TT, Gibson D, Painter GF, Kronenberg M, Zajonc DM (2010) Lipid binding orientation within CD1d affects recognition of Borrelia burgorferi antigens by NKT cells. *Proc Natl Acad Sci USA* **107:** 1535–1540

Wang X, Chen X, Rodenkirch L, Simonson W, Wernimont S, Ndonye RM, Veerapen N, Gibson D, Howell AR, Besra GS, Painter GF, Huttenlocher A, Gumperz JE (2008) Natural killer T-cell autoreactivity leads to a specialized activation state. *Blood* **112:** 4128–4138

Wesley JD, Robbins SH, Sidobre S, Kronenberg M, Terrizzi S, Brossay L (2005) Cutting edge: IFN-gamma signaling to macrophages is required for optimal Valpha14i NK T/NK cell cross-talk. *J Immunol* **174:** 3864–3868

Wun KS, Cameron G, Patel O, Pang SS, Pellicci DG, Sullivan LC, Keshipeddy S, Young MH, Uldrich AP, Thakur MS, Richardson SK, Howell AR, Illarionov PA, Brooks AG, Besra GS, McCluskey J, Gapin L, Porcelli SA, Godfrey DI, Rossjohn JA (2011) Molecular basis for the exquisite CD1d-restricted antigen specificity and functional responses of natural killer T cells. *Immunity* **34:** 327–339

Zajonc DM, Cantu III C, Mattner J, Zhou D, Savage PB, Bendelac A, Wilson IA, Teyton L (2005a) Structure and function of a potent agonist for the semi-invariant natural killer T cell receptor. *Nat Immunol* **6:** 810–818

Zajonc DM, Maricic I, Wu D, Halder R, Roy K, Wong CH, Kumar V, Wilson IA (2005b) Structural basis for CD1d presentation of a sulfatide derived from myelin and its implications for autoimmunity. *J Exp Med* **202:** 1517–1526